RADIAL MODE MATCHING ANALYSIS OF RIDGED CIRCULAR WAVEGUIDE

Uma Balaji and Ruediger Vahldieck

Laboratory for Lightwave Electronics, Microwaves and Communication
(LLiMiC)
Dept. of Elec. & Comp. Engg., University of Victoria, Victoria, B.C., Canada V8W 3P6

Abstract - Single ridged circular waveguides are useful for the development of compact septum polarizers. The design of these structures is based on the knowledge of modes in the semicircular and ridged waveguide sections. In this paper a radial mode matching analysis is presented to calculate rigourously the TE and TM modes that are excited in such a structure. Results are presented for variations of the ridge depth and ridge thickness and are compared to results from a finite element analysis.

1 Introduction

Application of ridged rectangular and circular waveguides can be found in many areas such as filters, matching circuits and polarizers. Recently, a compact polarizer has been developed with semicircular waveguide [1], similar to the stepped septum polarizer in square waveguide technology [2,3].

The optimum design of stepped septum polarizers requires the accurate calculation of the eigenvalues of the two orthogonal polarized modes for various heights of the single ridge. Furthermore, it is necessary to determine the onset of higher order modes that can possibly couple with the fundamental modes, because unwanted coupling between modes can significantly reduce port isolation. This was demonstrated in [1], where the dominant modes of the ridged circular waveguide have been calculated using the finite element method. In that work no higher order modes have been investigated and it was speculated that the moderate isolation between the two input ports (-26dB) of the polarizer can be attributed to coupling between the fundamental mode and TM_{01} mode. Since the finite element analysis is well known for spurious solutions, we have developed a radial mode matching technique to gain a better understanding of the behaviour of the higher order modes in such a structure. As a result of our analysis we have found that the third TE mode is significantly reduced and may also contribute to low isolation between both the polarizer ports.

2 Theory

The eigenvalues of the orthogonal dominant modes and higher order modes of the septum polarizer in circular waveguide can be obtained from the solution of the Helmholtz equation in cylindrical coordinates.

$$\frac{1}{\rho}\frac{\partial}{\partial\rho}(\rho\frac{\partial\psi}{\partial\rho})+\frac{1}{\rho^2}\frac{\partial^2\psi}{\partial\phi^2}+\frac{\partial^2\psi}{\partial z^2}+k^2\psi=0 \qquad (1)$$

In order to avoid numerical problems in dealing with structures of mixed coordinate system, the ridge or septum is cut radially for a thickness of 2θ [6]. This allows to bifurcate the structure into two subregions for which the potential functions can be written suitably. Using the separation of variables, we can define $k^2 = k_c^2 + k_z^2$ and hence the potential functions for regions 1 and 2 for TE modes, for the case of magnetic wall along the line of symmetry in Figure 1, can be written as follows

$$\psi^{(1)} = \sum_{n=1}^{N1} A_n J_n(k_c\rho)\sin n\phi \qquad (2)$$

$$\psi^{(2)} = \sum_{m=1,3}^{N2} C_m[H_l^{(2)'}(k_c a_2)H_l^{(1)}(k_c\rho)-$$

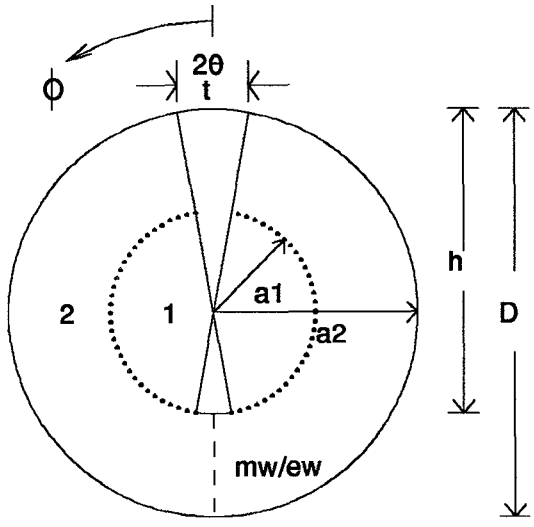

Figure 2: Single ridged Circular waveguide

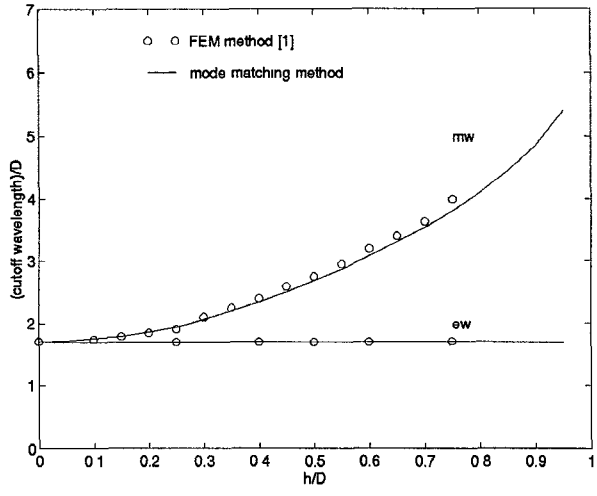

Figure 4: Cut-off characteristics of single ridged circular waveguide (t/D=0.04)

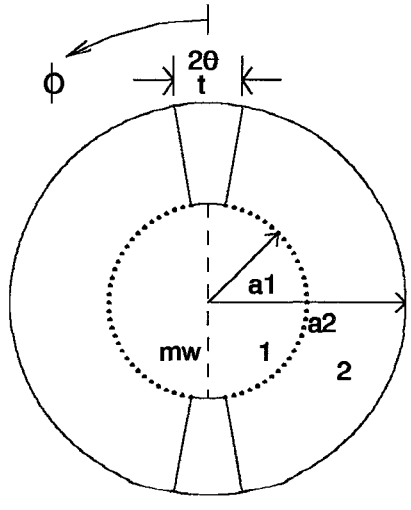

Figure 3: Double ridged Circular waveguide

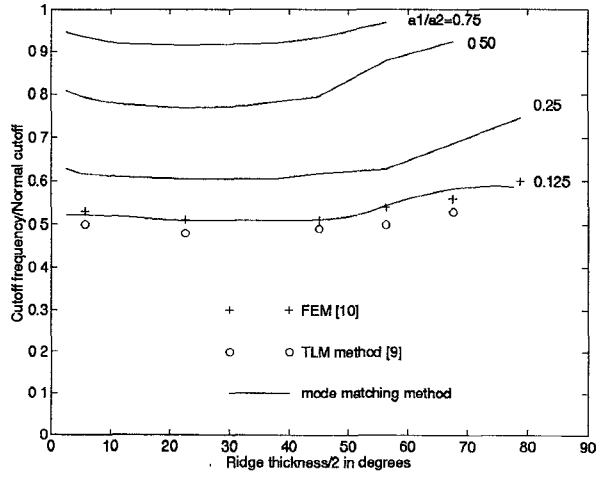

Figure 5: Cut-off characteristics of double ridged circular waveguide

3 Results

The eigenvalues for the fundamental mode of a single ridged circular waveguide have been evaluated using the above technique for the same dimensions as in reference [1]. The results shown in Figure 4 are in good agreement, even for the case where the ridge depth is larger than the radius of the circular waveguide. Depending on the polarization of this mode, the cutoff frequency either increases (horizontal polarization, ew) or decreases (vertical polarization, mw). The eigenvalues of some of the first higher order modes, for two different ridge parameters have been summarised in Table 1. It is clearly seen that the cutoff frequency for the TE_{31} mode is also significantly reduced by the ridge. The λ_c/D ratio of the TE_{31} mode changes from 0.75 for the circular waveguide ($a_1 = a_2$) to 1.04 for the case of $a_1 = 0.9a_2$. At the same time the cutoff frequency of TM_{01} mode increases.

The variation of the ratio of the cutoff frequency (TE_{11}) of double ridged circular waveguide to the normal cutoff of the circular waveguide as a function of the ridge parameter is shown in Figure 5 and resembles the behaviour in a rectangular waveguide. The detection of minimum singular values has been used for the determination of the eigenvalues as in [7]. It was found that $N1 = 5$ or 7 has been sufficient to produce results of good accuracy.

4 Conclusions

The radial mode matching technique has been developed to analyze circular ridge waveguide structures. In comparison to the finite element analysis the results are in good agreement for the fundamental mode. For the first time we have also presented results for higher order modes. Furthermore, by using conically shaped ridges, the problem of mixing rectangular and circular discontinuities has been avoided and all coupling integrals can be solved analytically. This measure makes the mode matching algorithm computationally very efficient.

References

[1] Roger Behe and Patrice Brachat, "Compact duplexer-polarizer with semicircular waveguide", IEEE Trans. A & P, vol. 39, pp. 1222-1224, Aug. 91.

[2] M. H. Chen and N. Tsandoulas, "A wide band square array polarizer", IEEE Trans. A & P, vol. 21, pp 389-391, May 1973.

[3] T. Ege and P. McAndrew, "Analysis of stepped septum Polarizers", Electronic Letters, Nov 1985, pp 1166-1168.

[4] R. F. Harrington, "Time-Harmonic Electromagnetic Fields", McGraw-Hill Book Co., 1961.

[5] S. Ramo, J. R. Whinnery and T. Van Duzer, "Fields and Waves in Communication Electronics", John Wiley and sons Inc. , 1965.

[6] B. V. de la Filolie and R. Vahldieck, "Coaxial and circular waveguide bandpass filters using printed metal inserts", IEEE MTT-S Digest, pp. 905 - 908, 1992.

[7] V. A. Labay and J. Bornemann, "Matrix singular value decomposition for pole free solutions of homogenous matrix equations as applied to numerical modelling", IEEE Microwave and guided wave letters, vol. 2, pp. 49-51, Feb. 92.

[8] J. Uher, J. Bornemann and U. Rosenberg, "Waveguide Components for antenna feed systems: Theory and CAD", Artech House inc. 1993.

[9] D.A. Al-Mukhtar, "Transmission-line matrix method with irregularly graded space", IEE Proc., Vol 128, Pt. H, No. 6, pp. 209-305, Dec 1981.

[10] Daly. P., "Polar geometry waveguides by finite element methods", IEEE Trans., MTT-22, pp. 202-209, 1974.

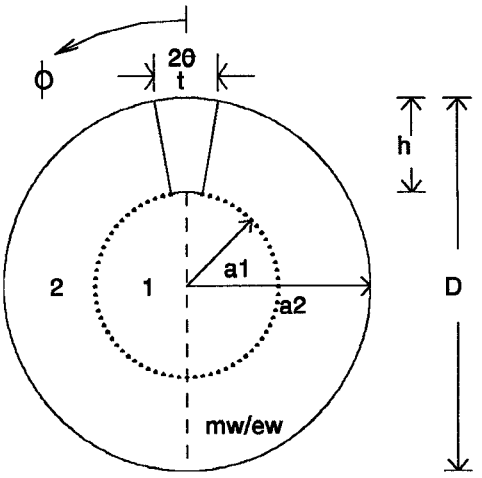

Figure 1: Single ridged Circular waveguide

Table. 1 (t/D=0.04)

Perturbed mode pattern	λ_c/D h/D=0.05	λ_c/D h/D=0.25
TE_{11}	1.7202	1.9430
TE_{31}	1.0446	1.2019
TE_{51}	0.7560	0.8484
TE_{12}	0.5896	0.5943
TE_{32}	0.4688	0.4777
TM_{01}	1.2887	1.1943

$$H_l^{(1)'}(k_c a_2) H_l^{(2)}(k_c \rho)] \cos l(\phi - \theta) \quad (3)$$

where, $l = \frac{m\pi}{2(\pi-\theta)}$. The functions J_n are the Bessel functions of order n and H_l are the Hankel functions of order l. The unknown coefficients of the eigenfunctions are A_n and C_m and a_2 is the radius of the circular waveguide.

The potential functions for the TM modes with a magnetic wall along the line of symmetry in Figure 1 is given by

$$\psi^{(1)} = \sum_{n=0}^{N1} B_n J_n(k_c \rho) \cos n\phi \quad (4)$$

$$\psi^{(2)} = \sum_{m=1,3}^{N2} D_m [H_l^{(2)}(k_c a_2) H_l^{(1)}(k_c \rho) -$$

$$H_l^{(1)}(k_c a_2) H_l^{(2)}(k_c \rho)] \sin l(\phi - \theta) \quad (5)$$

where, $l = \frac{m\pi}{2(\pi-\theta)}$.

The potential functions for the TE modes with an electric wall along the line of symmetry in Figure 1 is given by

$$\psi^{(1)} = \sum_{n=0}^{N1} A_n J_n(k_c \rho) \cos n\phi \quad (6)$$

$$\psi^{(2)} = \sum_{m=0}^{N2} C_m [H_l^{(2)'}(k_c a_2) H_l^{(1)}(k_c \rho) -$$

$$H_l^{(1)'}(k_c a_2) H_l^{(2)}(k_c \rho)] \cos l(\phi - \theta) \quad (7)$$

where, $l = \frac{m\pi}{(\pi-\theta)}$.

From the potential functions, the field components in each of the region can be derived. Equating E_ϕ and H_z along the radius a_1 for TE modes and E_z and H_ϕ for TM modes, over ϕ appropriately, and using orthogonality, a system of linear equations of infinite size as a function of k_c is obtained. The size of the system of equations is made finite depending on the truncation of the value of $N1$ and $N2$. The ratio between $N1$ and $N2$ is chosen to be close to the ratio of the angular widths of region 1 and region 2. The eigenvalue of the system, k_c is obtained either by searching for minimum singular value of the characteristic equation or by searching the zeros of the determinant. Since matrix singular value decomposition offers more accurate and pole free solutions [7], this technique has been chosen here for evaluation of the eigenvalues.

Special Case 1 : Ridge depth = Radius

The subregion 1 vanishes when the ridge depth is equal to the radius of the circular waveguide. The potential functions of the TE mode for this case is similar to [4].

$$\psi = J_n(k_c \rho) \cos n(\phi - \theta) \quad (8)$$

where, $n = 0, \frac{\pi}{2(\pi-\theta)}, \frac{2\pi}{2(\pi-\theta)} \ldots$.

The cutoff wavelength for the dominant and higher order modes in this case has been obtained from the search for the zeros of the function $J_n'(k_c a_2)$ as this makes $E_\phi = 0$ for $\rho = a_2$.

Special Case 2 : Ridge depth > Radius

When the ridge depth is greater than the radius of the circular waveguide as in Figure 2, the potential function for TE mode with magnetic wall along the line of symmetry is the same as equation 3 for region 2, while for region 1 it is

$$\psi^{(1)} = \sum_{n=0}^{N1} A_n J_q(k_c \rho) \cos \frac{n\pi(\phi - \theta)}{(\pi - 2\theta)} \quad (9)$$

where, $q = \frac{n\pi}{(\pi-2\theta)}$.

For the case of electric wall along the line of symmetry when the ridge depth is greater than the radius of the circular waveguide, the potential function for the region 1 will be the same as equation 9 and the potential function for region 2 will be the same as equation 7.

Similarly, expressions for potential functions for the TE modes of a double ridged circular waveguide (Figure 3) can be written as below. With a magnetic wall along the line of symmetry, the potential function for region 1 is the same as in equation 2, while for region 2 it is

$$\psi^{(2)} = \sum_{m=0}^{N2} C_m [H_l^{(2)'}(k_c a_2) H_l^{(1)}(k_c \rho) -$$

$$H_l^{(1)'}(k_c a_2) H_l^{(2)}(k_c \rho)] \cos l(\phi - \theta) \quad (10)$$

where, $l = \frac{m\pi}{(\pi-2\theta)}$.